Available online at www.sciencedirect.com
SCIENCE DIRECT
Catalysis Today 114 (2006) 403–411
CATALYSIS TODAY
www.elsevier.com/locate/cattod

The interaction of alumina with HCl: An infrared spectroscopy, temperature-programmed desorption and inelastic neutron scattering study

Alastair R. McInroy [a], David T. Lundie [a], John M. Winfield [a], Chris C. Dudman [b], Peter Jones [b], Stewart F. Parker [c], David Lennon [a,*]

[a] *Department of Chemistry, Joseph Black Building, The University of Glasgow, Glasgow G12 8QQ, UK*
[b] *Ineos Chlor Ltd., Runcorn Site HQ, South Parade, P.O. Box 9, Runcorn, Cheshire WA7 4JE, UK*
[c] *ISIS Facility, Rutherford Appleton Laboratory, Chilton, Didcot, Oxfordshire OX11 0QX, UK*

Available online 18 April 2006

Abstract

The interaction of HCl with an η-alumina catalyst has been investigated by a combination of diffuse reflectance infrared spectroscopy, temperature-programmed desorption and inelastic neutron scattering (INS) spectroscopy. Infrared spectra provide evidence for dissociative adsorption of HCl and for a process in which hydroxyl groups terminally bound to Al are replaced by chlorine. Temperature-programmed desorption experiments show HCl to desorb over the temperature range 350–>970 K, indicating dissociative HCl adsorption to occur on a wide range of active sites. INS experiments show the residual alumina hydroxyl groups to exhibit an out-of-plane deformation feature, γ(OH), at ca. 200 cm^{-1}, while the in-plane deformation mode, δ(OH), is seen at ca. 1000 cm^{-1}. The formation of new surface hydroxyl groups via the adsorption of hydrogen chloride yields a δ(OH) feature that can be resolved into two bands at 990 and 1050 cm^{-1}. Hydrogen bonding within the alumina/HCl system is responsible for the observation of an Evans transmission window in the infrared spectrum, that occurs via a Fermi resonance interaction between (i) the ν(OH) mode of hydrogen bonded hydroxyl groups and chemisorbed water with (ii) the overtone of the δ(OH) mode of surface hydroxyl groups. The INS technique is able to discriminate among different hydroxyl group bonding geometries on the basis of the local symmetry of the active sites.

Keywords: Alumina; Hydrogen chloride; Infrared spectroscopy; Temperature-programmed desorption; Inelastic neutron scattering

1. Introduction

Chlorination of alumina is relevant to the promotion of oxide and supported metal oxide catalysts [1,2] and also in the preparation of supported metal catalysts [3]. For example, Melchor et al. showed that the chlorination of alumina strengthened the Lewis acidity of the surface and produced a catalyst more active for the isomerisation of *n*-butane [4]. Chlorinated alumina catalysts have also been applied to the cracking of long chain alkanes [5] and the dehydrochlorination of chloroalkanes [1,2]. Chlorination can be achieved via the adsorption and subsequent reaction of various reagents such as tetrachloromethane [1,6], thionyl chloride [6], and hexachloroethane [6]. However, probably the most commonly studied system is that of HCl adsorbed on alumina [1,3,6–10]. This system also has importance in the industrial synthesis of methyl chloride, in which methanol and HCl are reacted over a suitable solid acid catalyst, normally alumina [11].

The adsorption of HCl on alumina is thought to occur via two distinct pathways. The first involves the dissociation of HCl onto aluminium oxygen pairs forming new hydroxyl groups and Al–Cl species (I). The formation of new hydroxyl groups has been confirmed from spectroscopic studies conducted by Peri [8] and Tanaka and Ogasawara [7], who observed broad hydroxyl bands at 3500 and 3400 cm^{-1}, respectively. The latter authors were able to show that the maximum absorbance of this new band was proportional to the amount of HCl adsorbed [7]. The second pathway also proceeds via dissociative adsorption of the HCl but with a hydroxyl exchange mechanism, where chlorine replaces a surface hydroxyl group coordinated to an aluminium ion (II).

* Corresponding author. Tel.: +44 141 330 4372; fax: +44 141 330 4888.
E-mail address: d.lennon@chem.gla.ac.uk (D. Lennon).

0920-5861/$ – see front matter
doi:10.1016/j.cattod.2006.02.041

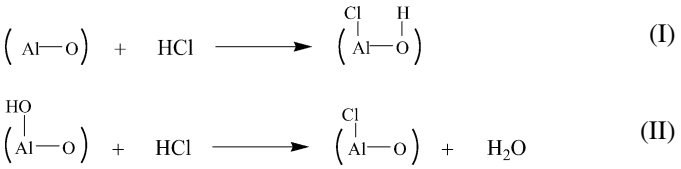

The former is thought to provide the main route to HCl adsorption, with the latter playing only a minor role [3,7,8].

Studies by Kytökivi et al. using a combination of infrared and NMR spectroscopies showed that determination of the ratio between the two processes was possible [3]. The alumina/HCl system has also been investigated from a theoretical perspective [10], that supports previous experimental findings [9]. It should be noted, that both these latter studies were carried out on a single crystal α-alumina (0 0 0 1) surface, an inherently simpler structure than that encountered when examining the technologically more relevant high surface area transition aluminas. The majority of studies carried out on this reaction system have been carried out on γ-alumina, since it has wide application in heterogeneous catalysis. Fewer studies have examined the same system on η-alumina, a naturally more acidic form of alumina [12,13], with applications in catalytic reforming reactions [14]. In the present paper, vibrational spectroscopy and temperature-programmed desorption (TPD) are used to investigate the interaction of HCl with an η-alumina catalyst, for which the surface acidity has recently been examined and characterised [15].

In the spirit of *operando* studies [16,17], initial characterisation experiments were performed using diffuse reflectance (DRIFTS) infrared spectroscopy [18]. These revealed an intense feature at $\sim$2100 cm^{-1}, the origin of which was not clear from inspection of the literature. In order to extend the accessible region of the vibrational spectrum, and thus aid a more complete assignment of the band about 2100 cm^{-1}, the adsorption state was also investigated using inelastic neutron scattering (INS) spectroscopy. This technique is proving to be increasingly important for extending the spectral range accessible in the examination of heterogeneous catalysts [19]. Recently, work from these laboratories has used this combination of techniques to characterise the interaction of methanol on η-alumina [20].

The application of infrared spectroscopy and INS presented here permits models of the adsorption process to be developed. Evidence for dissociative HCl adsorption plus both (i) hydroxyl group formation and (ii) the hydroxyl group exchange mechanism is observed. Aspects of these processes are considered within the context of a recently described model for the surface acidity of η-alumina [15].

2. Experimental

2.1. Catalyst characterisation and general procedures

The η-alumina examined is a commercial grade catalyst [21], that has application in the synthesis of methyl chloride from the reaction of methanol and hydrogen chloride [22]. Characterisation of the catalyst (BET surface area = 328 $\pm$ 29 $m^2\ g^{-1}$, pore volume = 0.34 $\pm$ 0.04 $cm^3\ g^{-1}$) has been described elsewhere [15]. The η-alumina sample was activated by heating to 623 K under flowing helium (BOC, 99.999%) for 150 min, then allowed to cool to ambient temperature. For infrared and TPD experiments, the sample was flushed continuously with helium gas, fed to the catalyst via an in-line gas purification system (Messer Greisheim Oxisorb). These experiments were performed at least in duplicate. For the INS experiments high purity helium (BOC, 99.999%) was used as a carrier gas but no in-line purification was employed.

2.2. Infrared spectroscopy

Infrared experiments were performed using a Nicolet Nexus FTIR spectrometer fitted with a MCT high D^* detector. A SpectraTech Smart diffuse reflectance cell and environmental chamber were used for diffuse reflectance measurements, using a typical sample size of 30–50 mg. The sample cell was connected to a vacuum manifold/gas flow apparatus that provided control of the flow of gases into the infrared cell. This included an in-line sample loop for sequential dosing of the catalyst in a pulse-flow arrangement. The exit stream of the infrared cell could be monitored by a quadrupole mass spectrometer (LedaMass LM22). A constant stream of high purity helium was passed over the catalyst at all times (30 ml min^{-1}, 1.5 bar). The sample was activated in situ. Background spectra were recorded post-activation at 293 K. HCl (Linde Gas, purity >99%), was dosed to the catalyst at 293 K using pulse-flow techniques [23,24]. Ancillary experiments confirmed that a 5 min delay after each dosing pulse was sufficient time for the adsorbate to be removed completely from the environmental chamber. After dosing, the spectrum was recorded (128 scans, 2 cm^{-1} resolution). All spectra are presented as background subtractions, where a spectrum of the activated catalyst has been subtracted from the dosed spectrum. No baseline or offset corrections were made. For HCl desorption experiments, the cell containing the pre-dosed catalyst sample was heated under flowing He. The cell was maintained at a specified temperature for 15 min, before being cooled to room temperature where a spectrum was recorded.

2.3. Temperature-programmed desorption

A detailed description of the experimental set up employed for thermal desorption experiments has been given elsewhere [15]. Experiments were performed with the catalyst sample contained within a packed bed tubular reactor (0.25″ stainless steel tubing) located within a temperature programmable oven (Neytech 25 PAF). A mass spectrometer (Leda Mass LM22, closed ion source) sampled the eluting gases via a differentially pumped capillary line and a sintered-metal precision leak. The alumina sample was activated and dosed with HCl as outlined above. Saturation of the sample could be observed by monitoring the eluant stream on the mass spectrometer. When saturation was achieved, the sample was left to purge overnight at 293 K under flowing He. This procedure was intended to purge physisorbed HCl from the alumina surface. TPD

experiments were performed at a temperature ramp rate of 8 K min^{-1}. The HCl signal from the reactor was monitored by the mass spectrometer at all times during the TPD experiment. During some of the TPD experiments, the mass spectrometer was also tuned to dichlorine but no significant signals were observed, indicating HCl to be the dominant desorption product, with recombination of chemisorbed chlorine atoms playing no role in the thermally induced surface chemistry.

2.4. Inelastic neutron spectroscopy

Inelastic neutron scattering experiments were performed using the MARI spectrometer [25] at the ISIS pulsed spallation neutron facility at the Rutherford Appleton Laboratory. For HCl adsorption, alumina (ca. 18 g) contained in a stainless steel INS cell was activated as above, then allowed to cool in flowing helium to 300 K. The sample was then connected to a vacuum manifold, evacuated, and then isolated. HCl was exposed to the catalyst in increasing aliquots up to an equilibrium pressure of 500 mbar. Initial exposures were performed slowly due to the considerable exotherm associated with this reaction. The sample then remained under a pressure of 500 mbar for 20 min before being isolated and removed to the spectrometer. The sample cell was connected to a closed cycle refrigerator and cooled to below 20 K, at which temperature the INS spectrum was acquired.

3. Results and discussion

3.1. Infrared spectroscopy

The background subtracted, diffuse reflectance infrared spectrum for a saturated overlayer of HCl adsorbed on η-alumina is shown in Fig. 1. The broad intense band at ca. 2720 cm^{-1} represents molecular HCl, and is assigned to the H–Cl stretch. Hydrogen chloride in the gaseous and liquid phase exhibit an absorption at, respectively 2886 and 2785 cm^{-1} [26,27]. The reduction in wavenumber seen in Fig. 1 is believed to reflect some overlap from adjacent bands plus a shift in the frequency position for the H–Cl stretch due to interaction of the HCl molecule with the lattice. Molecular HCl is normally not observed in infrared studies of HCl on alumina, due to the predominance of dissociative adsorption [8]. The molecular HCl apparent in Fig. 1 could represent physisorbed material, which has not been removed by the purge routine. Alternatively, it could also reflect a contribution from associatively bound HCl. Thermal desorption studies described below indicate this species to be weakly bound.

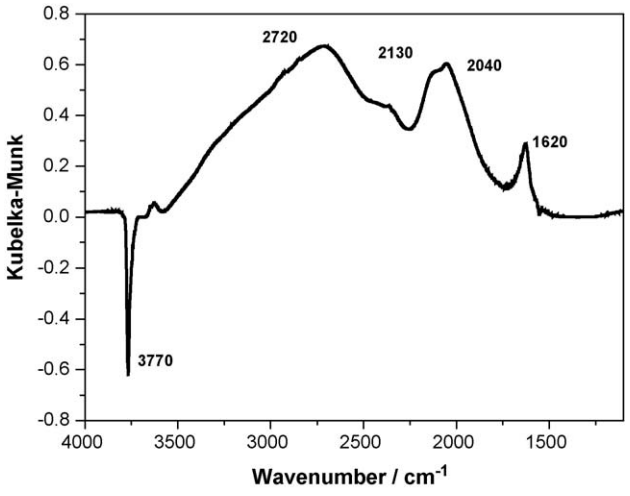

Fig. 1. The background subtracted diffuse reflectance spectrum for a saturated overlayer of HCl on η-alumina at 293 K.

The HCl feature exhibits a broad shoulder at ca. 3300 cm^{-1}, which corresponds to the (O–H) stretch of hydrogen bonded OH groups, consistent with previous studies [7,8]. Two entities could contribute to this feature: hydroxyl groups formed via dissociative HCl adsorption (I), or water molecules formed via dissociative HCl adsorption accompanied by a hydroxyl exchange process (II). The presence of water is confirmed by the strong (O–H) deformation band at 1620 cm^{-1}. A relatively low intensity peak at ca. 3600 cm^{-1} is also present which indicates that a small number of ''free'', non-hydrogen bonded hydroxyl groups are also formed via Eq. (I) [28].

Fig. 1 is characterised also by the presence of an intense feature of negative intensity at ca. 3750 cm^{-1}, which is comprised of a sharp peak at 3770 cm^{-1} and a shoulder at 3730 cm^{-1}. An analogous feature has been reported previously in the diffuse reflectance spectra for pyridine [15,29] and methanol [20] on alumina. In these cases it is attributed to a hydrogen bonding interaction between isolated surface hydroxyl groups and the adsorbate, that is bound via an adjacent coordinatively unsaturated aluminium ion [15,20]. However, despite the similarities, a comparable process is not thought to be active on this occasion. In the previous studies no water was formed, establishing that a replacement mechanism was inactive, and yet Fig. 1 shows clear evidence for the formation of water, presumably via dissociative HCl adsorption and the hydroxyl group exchange process (II). This is the dominant route for water formation, as the dissociative adsorption plus hydroxyl formation pathway (I) produces only surface hydroxyl groups. Thus, the sharp feature at 3750 cm^{-1} is interpreted as arising from the loss of non-hydrogen bonded hydroxyl groups that occurs via the dissociative adsorption of HCl and the associated replacement with a chemisorbed chlorine atom, i.e. process (II). It should be noted that infrared spectroscopy does not provide any direct confirmation for the dissociative adsorption process, as the resulting Al–Cl stretch is below the alumina ''cut-off'' frequency in diffuse reflectance measurements of ca. 1200 cm^{-1} [20].

Fig. 1 also shows an intense band at ca. 2100 cm^{-1}, which is comprised of two peaks centred at 2040 and 2130 cm^{-1}. To the knowledge of the authors, and despite its dominant presence in Fig. 1, this feature has not previously been reported for HCl on alumina. Rather than reflecting a discrete mode of, possibly, a new surface species, this feature is considered to be associated with an Evans transmission window. This phenomenon occurs when a broad ν(OH) envelope overlaps with the overtone of a hydroxyl deformation mode and experiences a Fermi resonance interaction [30]. Claydon and

Sheppard demonstrated the effect experimentally in hydrogen bonded solids [31], whilst Bratos and Ratajczak used a stochastic approach to define the band profiles observed in strongly hydrogen bonded systems [32]. Subsequent work by Pelmenschikov and co-workers examining zeolitic H complexes established the effect could also be observed for chemisorbed systems [33] and Kubelková et al. applied Fermi resonance theory to reproduce spectral patterns observed by transmission FTIR for surface complexes in zeolites of various acidities [34]. The feature in Fig. 1 exhibits an ''A, B'' type profile [31,33], with peak A centred about 2700 cm^{-1} and peak B centred at ca. 2100 cm^{-1}. The ''dip'' between these features appears at ca. 2257 cm^{-1}, which should correspond to the first overtone of a δ(OH) feature; the latter is unobservable in Fig. 1 as it resides below the alumina ''cut-off'' value.

In order to gain an improved understanding of the nature of the intense feature at ca. 2100 cm^{-1}, the infrared spectrum of the saturated overlayer was monitored as a function of temperature. The data are presented in Fig. 2. Heating the sample to 423 K (Fig. 2(a)(ii)), resulted in the concomitant loss in intensity of the peaks associated with molecular HCl (ν(H–Cl, 2795 cm^{-1}), water (ν(O–H), ca. 3300 cm^{-1} and δ(O–H), 1620 cm^{-1}), and the broad band at ca. 2100 cm^{-1}. The separation between the ν(O–H) of water and the ν(H–Cl) of HCl is more apparent at this stage. The HCl feature now exhibits a peak maximum at ca. 2795 cm^{-1}, which is closer to the liquid phase frequency of 2785 cm^{-1} [27]. Evidently, the reduction in the intensity of the adjacent ν(O–H) feature has permitted a more reliable observation of the vibrational frequency for this oscillator.

The free hydroxyl region of the spectrum is presented in Fig. 2(b), where a reduction in intensity for the small feature at

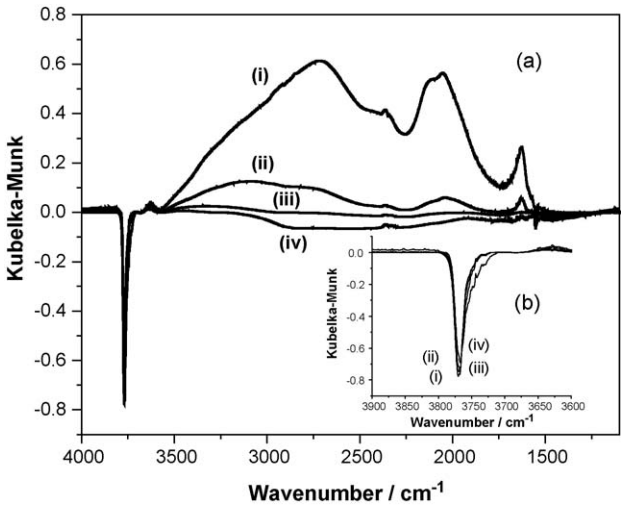

Fig. 2. Diffuse reflectance spectra as a function of temperature of a saturated chemisorbed overlayer of HCl: (a) 4000–1200 cm^{-1} and (b) the free hydroxyl region. (i) Saturation spectrum dosed at 293 K. The sample was then progressively warmed to (ii) 423, (iii) 523, and (iv) 623 K. A flow of He was continually passed over the sample while heating to progressively higher temperatures. The sample was held at the desorption temperature for 15 min and then allowed to cool to room temperature, where the spectrum was acquired. All spectra are background subtracted, where the spectrum of the clean activated catalyst has been subtracted from the measured spectrum.

ca. 3600 cm^{-1} and a significant narrowing of the sharp negative band at 3770 cm^{-1} are both observed. Further warming to 523 K leads to an essentially flat baseline, with the noticeable exception of the sharp peak at 3770 cm^{-1}. The intensity and lineshape of this distinct feature is effectively unchanged upon further warming to 623 K. Thus it appears that water, HCl and the species responsible for the broad feature at ca. 2100 cm^{-1} desorb from the surface over a comparable temperature range, with desorption complete by ca. 523 K. Observation of this trend in the spectra raises the possibility that the unassigned peak could be associated with HCl. However, ca. 2100 cm^{-1} represents a decrease in vibrational frequency of >800 cm^{-1} from that of molecular HCl, which seems unlikely, suggesting that this feature is not due to HCl residing in special sites or experiencing strong hydrogen bonding interactions at the surface.

The 2100 cm^{-1} band in Fig. 1 resembles an anomalous feature at 2600 cm^{-1} recently reported for methanol on η-alumina; the latter has been assigned to a combination of the methyl rock and methyl deformation modes of chemisorbed methoxy groups [20]. However, the temperature dependence of the 2100 cm^{-1} band contrasts significantly with the 2600 cm^{-1} band of methanol on η-alumina. Whereas Fig. 2 indicates the intensity of the 2100 cm^{-1} band to diminish on heating at a rate comparable to that of the ν(OH) feature, the methanol derived band at 2600 cm^{-1} remains on thermal treatment that significantly reduces the ν(OH) feature [20]. Thus, temperature-programmed infrared spectroscopic measurements indicate the 2100 cm^{-1} feature to be linked to the hydroxyl stretch (associated with hydrogen bonded hydroxyl groups and chemisorbed water molecules). It appears not to constitute a separate molecular entity, as was found for methanol on alumina.

In Fig. 2(b), the frequency position of the sharp negative intensity band in the background subtracted spectrum provides information on the nature of the site experiencing the exchange of hydroxyl groups by chemisorbed chlorine. Previous studies by the authors on this substrate have correlated the surface acid site distribution with the hydroxyl stretching frequencies and report a frequency of 3770 cm^{-1} to correspond to a medium–strong Lewis acid site and a band at 3730 cm^{-1} to be associated with a medium–weak Lewis acid site [15]. On this basis, the shoulder at 3730 cm^{-1} in Fig. 2(b) represents a small loss of hydroxyl groups from the medium–weak Lewis acid sites that are recovered on warming to 423 K. More significantly, however, Fig. 2(b) shows the medium–strong Lewis acid site to dominate and this feature remains effectively unchanged even after heating to 623 K. Its narrow linewidth (FWHM = 16 cm^{-1} after warming to 623 K) is indicative of a single molecular entity exhibiting a high degree of local order. Fig. 3 presents a schematic representation of the medium–strong Lewis acid site [15] and outlines schematically the dissociative adsorption of HCl and the hydroxyl exchange process that leads to the loss of water (process (II)). Interestingly, such a transformation leads to the regeneration of an active site. This is an elaboration of process (II) [3], in that it indicates dissociative adsorption of HCl to precede the OH/Cl exchange process. Moreover, Fig. 3 indicates that, due to the increased electronegativity of the

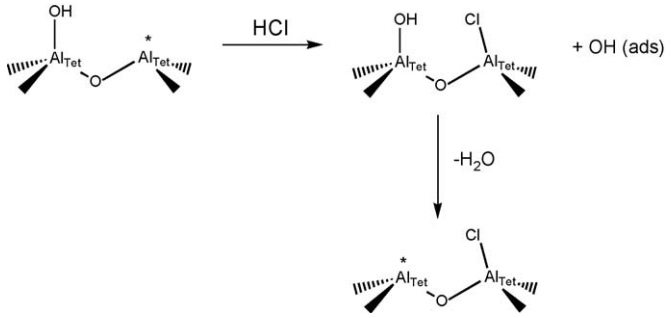

Fig. 3. A schematic representation of the adsorption of HCl at a medium–strong Lewis acid site [15] and the effect of subsequent H_2O loss. The asterisks indicate coordinative unsaturation.

chlorine relative to a hydroxyl group, the newly generated Lewis acid site will be more acidic than the original. This approach therefore indicates that chlorination via HCl should lead to enhanced Lewis acidity and is entirely consistent with the findings reported by Melchor et al. [4].

Fig. 2(b) indicates that the OH/Cl replacement process occurs to a significant extent only at the medium–strong Lewis acid site. Of the four active sites proposed in our earlier work [15], this is the only one with an adjacent terminal hydroxyl group. The weak and medium–weak Lewis acid sites are associated respectively with three- and two-fold hydroxyl groups adjacent to the coordinating Al centre. Multiple coordination implies a higher binding energy and thus it is possible that the replacement mechanism is accessible only for isolated terminally bound hydroxyls (medium–strong Lewis acid sites) and energetically inaccessible for non-hydrogen bonded bridging hydroxyl groups. Kytökivi et al. have observed a similar trend for HCl adsorption on γ-alumina [3].

3.2. Temperature-programmed desorption

Fig. 4 presents the temperature-programmed desorption spectrum obtained for HCl adsorbed on η-alumina and shows a broad desorption profile ranging from ca. 360 K to in excess of 950 K. TPD studies for HCl on a single crystal α-alumina (0 0 0 1) surface typically yield smooth unstructured desorption curves from 300 to 650 K, although pre-treatments can give rise to two separate states [9]. The higher desorption temperatures seen in Fig. 4 reflect the greater surface complexity and wider range of active sites present with η-alumina; these are as a result of the different structural/coordinative features of the two phases [35].

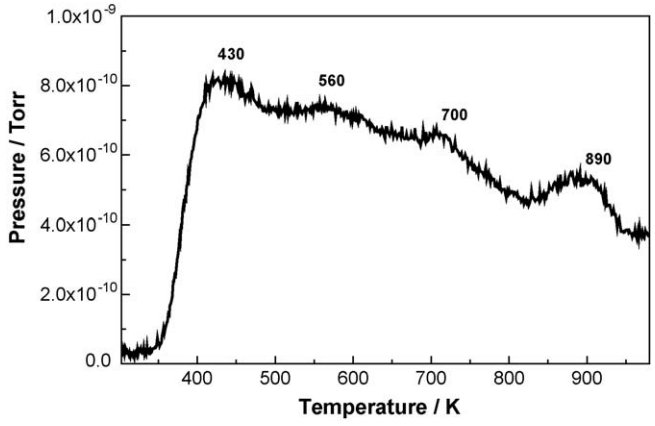

Fig. 4. Temperature programmed-desorption spectrum for a saturation chemisorption dose of HCl on η-alumina. The sample was maintained at 293 K and dosed with repeated pulses of HCl until the mass spectrometer detected no further retention of adsorbate by the catalyst. The sample was then purged overnight to remove any physisorbed HCl. The HCl mass spectrometer signal was monitored as a temperature gradient of 8 K min^{-1} was applied up to 1000 K.

Closer inspection of Fig. 4 reveals some fine structure to be contained within the broad envelope of the TPD spectrum, with peaks discernible at 430, 560, 700, and 890 K. These TPD experiments were repeated on three separate occasions and Fig. 4 is representative of the spectra. The observation that the TPD profile can be sub-divided into four states is coincident with the assignment of surface acidity to four distinct sites [15]. Following this possibility through, the TPD features are assigned as follows: 430 (weak Lewis acid site), 560 (medium–weak Lewis acid site), 700 (medium–strong Lewis acid site), and 890 K (strong Lewis acid site). It is should be borne in mind that although chlorine will bind to the coordinatively unsaturated aluminium sites, hydrogen is expected to go to an adjacent, but unspecified, oxygen.

Fig. 2 indicates the absence of molecular HCl from the surface after warming to 523 K. Fig. 4 clearly shows HCl desorption from 350 to >970 K. Molecular adsorption of HCl is not expected to displace surface hydroxyl groups, neither should it produce water molecules. Therefore, Fig. 4 represents desorption from dissociatevely adsorbed HCl. Furthermore, it indicates that the resulting chlorine atoms bind to all four Lewis acid sites identified in a previous examination of this substrate [15].

3.3. Inelastic neutron spectroscopy

Fig. 5 presents the INS spectrum for activated alumina recorded using the MARI spectrometer operating at incident energies of (a) 4840 and (b) 1290 cm^{-1}. Spectral resolution on this instrument is related to the incident energy selected [20], so recording spectra over two energy ranges means

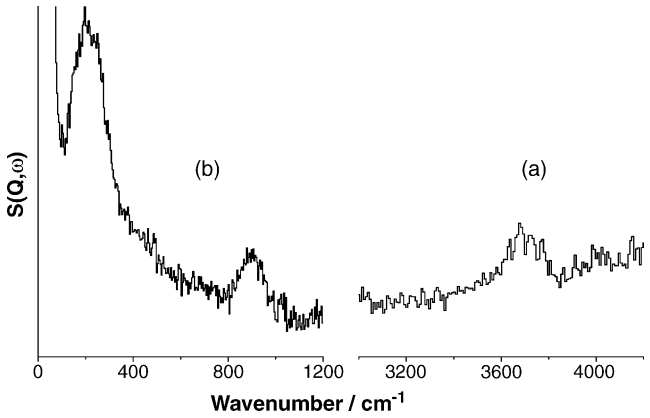

Fig. 5. INS spectra of the η-alumina catalyst after activation at 623 K recorded using the MARI spectrometer with an incident energy of (a) 4840 cm^{-1} (3000–4200 cm^{-1}) and (b) 1290 cm^{-1} (50–1200 cm^{-1}).

reasonable resolution can be maintained over a wider spectral range than that obtainable at a single energy [36]. A broad feature about 3700 cm^{-1} that ranges from ca. 3600 to 3800 cm^{-1} with a maximum at 3676 cm^{-1} is assigned to the OH stretch of hydroxyl groups present at the alumina surface. The peak at 905 cm^{-1} is assigned to the deformation mode of surface hydroxyl groups [37–39]. This mode is generic to all hydroxyls. However, for the terminal hydroxyl group associated with the medium–strong site as depicted in Fig. 3, this feature represents an in-plane hydroxyl deformation, δ(OH). The intense feature at ca. 200 cm^{-1} is assigned to the out-of-plane deformation of surface hydroxyl groups, γ(OH). This mode approximates to a torsional motion of the hydroxyl group [40]. Such modes normally yield intense features in INS spectra [36].

It is noted that the δ(OH) and γ(OH) modes of alumina are not normally accessible in infrared spectroscopy and Fig. 5 indicates the benefit of applying INS to characterise such economically relevant catalytic substrates. However, in favourable circumstances, these modes can be accessed on other high surface area oxides of relevance to heterogeneous catalysis. For instance, the δ(OH) mode can be attainable in zeolitic materials [33], although normally the γ(OH) mode cannot be observed. A notable exception is the use of far infrared spectroscopy by Hoffman and Knözinger to reveal the position of the γ(OH) mode for silica [40]. Nevertheless, the direct observation of both hydroxyl deformation modes for alumina by INS represents a substantial advance, that assists greatly the evaluation of the contribution of non-fundamental modes to the vibrational spectrum, as observed in conventional mid-infrared experiments (e.g. Fig. 1).

INS spectra for the chemisorbed overlayer recorded at an incident energy of 2420 cm^{-1} are presented in Fig. 6. This spectral range focuses on the deformation modes, with Fig. 6(a) showing the background spectrum. At this incident energy only the γ(OH) deformation of the surface hydroxyl groups is apparent at 200 cm^{-1}; the δ(OH) mode is observed as a weak, broad feature at ∼900 cm^{-1}. The spectrum for the HCl dosed catalyst is shown in Fig. 6(b), which shows increases in intensity at 1640 and 905 cm^{-1}, associated respectively with the formation of water via process (II) and hydroxyl groups by process (I). However, the γ(OH) deformation band at ca. 200 cm^{-1} shows a modest reduction in intensity in Fig. 6(b) compared with the background. This aspect of the adsorption process is made clearer by examination of the background subtracted spectrum (Fig. 6(c)), which shows a "dip" in scattering intensity at about 200 cm^{-1}. This indicates a loss of hydroxyl groups present in this environment, consistent with Fig. 1 and process (II) and as depicted in Fig. 3. The apparent absence in Fig. 6(c) of the feature at ca. 2100 cm^{-1} that contributes strongly to the diffuse reflectance spectrum for a saturated overlayer of HCl (Figs. 1 and 2) indicates this state could possibly be non-hydrogenic or, more likely, it is inherently weak in INS due to a low amplitude of motion.

In an attempt to gain further insight into the trends observed in Fig. 6, spectra were acquired at improved resolution by using an incident energy of 1290 cm^{-1} and are presented in Fig. 7. The hydroxyl δ(OH) and γ(OH) modes are now clearly observable in the background spectrum at ca. 900 and 210 cm^{-1}, respectively. The HCl dosed spectrum, Fig. 7(b), shows some attenuation of the γ(OH) feature at ca. 210 cm^{-1} and changes are apparent in the δ(OH) region, particularly about 1000 cm^{-1}, indicating a shift to higher wavenumber for this feature. The background subtracted spectrum, Fig. 7(c), demonstrates these perturbations to the hydroxyl signals more clearly. The negative inflection about 180–210 cm^{-1} confirms the loss of hydroxyl groups contributing to the γ(OH) mode. A broad feature at ca. 550 cm^{-1} is discernible; this is assigned to the librational mode of water [41], which is formed as a consequence of process (II). In addition, the hydroxyl deformation mode shows an increase in intensity at ca. 1000 cm^{-1}, which is resolvable into two peaks at 990 and 1050 cm^{-1}. Previously, Kubelková et al. have shown that adsorption of probe molecules involving hydrogen-bonding interactions in zeolites lead to an increase in frequency of substrate hydroxyl bending modes [34]. Formation of hydroxyl groups, via process

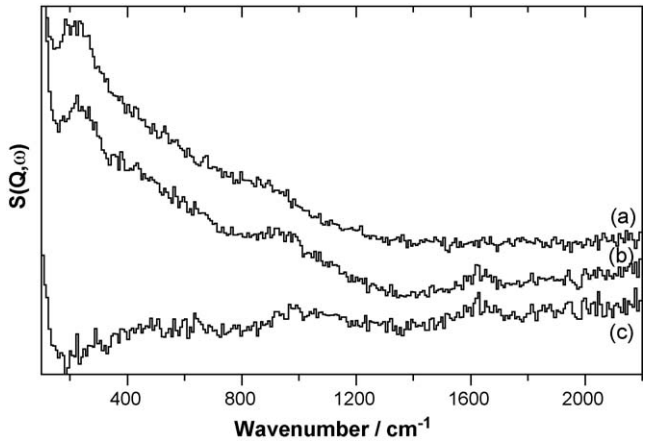

Fig. 6. INS spectra recorded using the MARI spectrometer with an incident energy of 2420 cm^{-1} for (a) the η-alumina background and (b) a saturated chemisorbed overlayer of HCl on η-alumina, and (c) the difference spectrum (b) − (a).

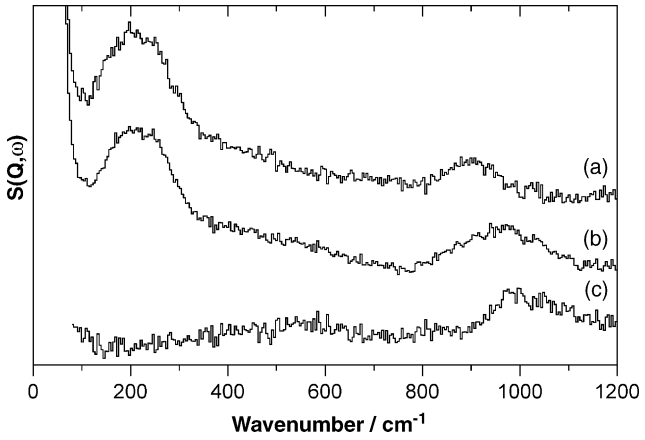

Fig. 7. INS spectra recorded using the MARI spectrometer with an incident energy of 1280 cm^{-1} for (a) the η-alumina background and (b) a saturated chemisorbed overlayer of HCl on η-alumina, and (c) the difference spectrum (b) − (a).

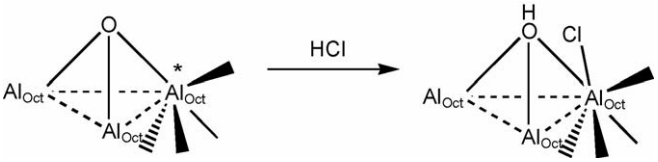

Fig. 8. Schematic representation of HCl dissociatively adsorbed at a coordinatively unsaturated aluminium site (★) with the adjacent oxygen atom exhibiting three-fold coordination. This site approximates to the weak Lewis acid site [15].

(I), will lead to a positive feature about 1000 cm^{-1}, which is attributed to the (OH) deformation mode [37–39].

These trends revealed in the INS spectra provide information on HCl adsorption at coordinatively unsaturated aluminium sites with adjacent oxygen atoms exhibiting three-fold coordination. Such sites approximate to the weak Lewis acid site described elsewhere [15], although in this instance the bridging oxygen atom is not bonded to a hydrogen. One of the adsorption processes postulated is presented schematically in Fig. 8. The hydroxyl group exhibits pseudo-C_{3v} symmetry. The deformation mode for the C_{3v} point group is doubly degenerate, however, under the pseudo-C_{3v} symmetry encountered at this site, the degeneracy will be partially lifted, leading to two peaks associated with this mode. This small splitting, as evidenced by the peaks at 990 and 1050 cm^{-1} in Fig. 7(c), can apply only to hydroxyls associated with triply-coordinated oxygen atoms. The terminal hydroxyl that is consumed in process (II), as illustrated in Fig. 3, will therefore also show a loss of intensity in the associated in-plane deformation. Fig. 5 shows this mode occurs at ca. 905 cm^{-1} and so the expected negative inflection related to process (II) is believed to be masked in Fig. 7(c). This is a consequence of the increase in intensity in this region due to the production of hydroxyls formed via process (I). Interestingly, the INS spectra presented here are able to discriminate between different hydroxyl bonding geometries on the basis of the local symmetry at the active sites.

3.4. Correlation between IR and INS

The INS spectra complement the infrared spectra and provide the basis for confirming the origin of the anomalous feature in the diffuse reflectance spectrum at ca. 2100 cm^{-1}. Fig. 7 identifies the δ(OH) mode of surface hydroxyl groups formed from the dissociative adsorption of HCl to yield a signal at ca. 1050 cm^{-1}. The first overtone of this feature will therefore occur about 2100 cm^{-1}, which is a reasonable match to the minimum in the transmission window at 2257 cm^{-1} in Fig. 1. In principle, the wavenumber of the minimum in an "A, B" Evans window should correspond to the wavenumber of the first harmonic [31], i.e. 2100 cm^{-1}. However, the Evans window is a result of a redistribution of the infrared intensity between ν(OH) and 2δ(OH) modes that are shifted as a consequence of hydrogen bonding interactions. Kubelková et al. have demonstrated that the centre of the window is at the frequency of the 2 × δ(OH) value only if the A and B features have the same integrated intensity [34]. The fact that 2 × δ(OH) ≠ 2257 cm^{-1} is a reflection of the proportionally greater intensity of the A lobe in Fig. 1. The position of the minimum indicates the extent of the hydrogen bonding, with increased hydrogen bonding shifting the minimum to lower wavenumber [34].

Further inspection of Fig. 1 shows the 2100 cm^{-1} peak to be comprised of two bands at 2130 and 2040 cm^{-1}, with a minimum at 2091 cm^{-1}. Two assignments are possible here. Firstly, the 2100 cm^{-1} peak could result from a combination mode and an overtone of the δ(OH) features seen in Fig. 7(c), that are formed via process (I). Specifically, a combination of the δ(OH) features at 990 + 1050 cm^{-1} will lead to a band at ca. 2040 cm^{-1} and an overtone of the δ(OH) feature at 1050 cm^{-1} will lead to a band at ca. 2100 cm^{-1}. These predicted wavenumbers are in reasonable agreement with the doublet observed in the infrared spectrum (Fig. 1). However, it is also possible that the ca. 2100 cm^{-1} features represents another Evans window, with the 2130 and 2040 cm^{-1} maxima representing a further manifold of A and B type bands, that is superimposed on the low wavenumber tail of the hydrogen bonded ν(OH) signal. Fig. 7(c) shows the δ(OH) of hydroxyl groups formed via equation (I) to exhibit a peak maximum at ca. 1000 cm^{-1}. In addition to the overtone of the residual δ(OH) mode leading to the "dip" in Fig. 1 at 2257 cm^{-1}, it is possible that a combination of the two δ(OH) peaks could also be interacting via Fermi resonance to yield the observed minimum at 2091 cm^{-1}: 990 + 1050 cm^{-1} = 2040 cm^{-1}, which is close to the observed value. The similarity of these values is attributed to the nearly symmetric nature of the two lobes at this energy. Further work, including transmission infrared experiments, is necessary to refine the precise assignment for this band. Nevertheless, despite some uncertainty in establishing whether the 2100 cm^{-1} feature is comprised of two peaks or it actually represents pseudo-maxima, it is apparent that it is intimately connected to the δ(OH) features seen in Fig. 7(c) and that it does not represent a separate molecular entity.

A feature of neutron spectrometers such as MARI, is that they measure the scattered neutron intensity (S) as a function of both energy (ω, cm^{-1}) and momentum (Q, $Å^{-1}$) [36]. This

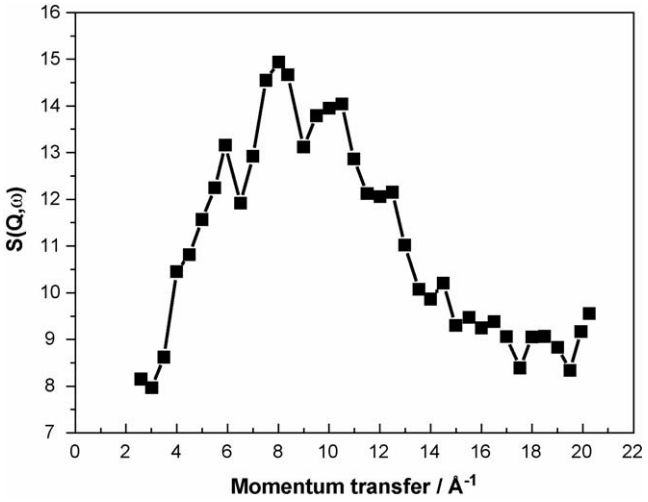

Fig. 9. The momentum transfer dependence of the modes at 900–1000 cm^{-1} for the chemisorbed HCl sample.

capability can be exploited to determine whether a particular vibrational feature is a fundamental mode ($n = 1$), or whether it corresponds to a higher order transition ($n \geq 2$) [20]. Fig. 9 shows the Q dependence of the δ(OH) mode at 900–1000 cm^{-1}, where it peaks at about 8 $Å^{-1}$. Previous work by Parker et al. has shown that the maximum of the S versus Q plot ($dS/dQ \approx 0$) indicates the order of the vibrational transition [42]. A value of 8 $Å^{-1}$ is indicative of a $n = 1$ transition [20], confirming this mode to be a fundamental. Given the inherent low intensity of the fundamental, it is understandable why the higher order transitions are not apparent in Fig. 6. This analysis confirms the band at ca. 1000 cm^{-1} to constitute a fundamental mode, which further strengthens the explanation of this mode interacting with the ν(OH) feature to lead to the somewhat atypical band profile seen in Fig. 1.

Against this heightened appreciation of the interactions between hydroxyl modes leading to significant perturbations of the observed infrared spectrum, it is worthwhile to re-examine the spectral profile depicted in Fig. 1. Strongly hydrogen bonded systems can lead to "A, B, C" as well as "A, B" type spectra [31], with the "C" feature conferring a pseudo-maximum at ca. 1700 cm^{-1} in zeolitic systems [33]. It is possible that the band maximum at 1620 cm^{-1} could correspond to a "C" band, with a minimum between the "B" (2100 cm^{-1}) and "C" bands seen at 1734 cm^{-1}. For such an Evans hole, this minimum is generally associated with overlap between ν(OH) and 2γ(OH) [31]. Now Figs. 5–7 show γ(OH) to occur at ca. 200 cm^{-1}, a transition energy far to low for the first harmonic to overlap with ν(OH) to lead to an Evans window. Thus, Fig. 1 exhibits an "A, B" and not an "A, B, C" spectral profile, where the 1620 cm^{-1} band assignment is confirmed as arising from the δ(OH) mode of chemisorbed water, formed via process (II), that exhibits a strong hydrogen bonding interaction with the alumina surface so as to shift the ν(OH) band envelope to low wavenumber.

4. Conclusions

An examination of the η-alumina/HCl adsorption system has been made using a combination of infrared spectroscopy, temperature-programmed desorption and INS spectroscopy. The main conclusions can be summarised as follows:

- Infrared data provide evidence for the replacement of surface hydroxyl groups by chlorine and the formation of water. These observations are consistent with dissociative HCl adsorption leading to Al–Cl formation plus (i) hydroxyl group formation and (ii) a hydroxyl exchange reaction which liberates water. Molecular HCl is also evident, as is a previously unreported intense feature at ca. 2100 cm^{-1}.
- The TPD profile shows HCl to desorb over the temperature range 350–>970 K, indicating dissociative HCl adsorption to occur on a wide range of active sites. Fine structure in the TPD spectrum can be associated with adsorption of chlorine with the four types of Lewis acid site previously reported for this surface [15], with the associated hydrogen adsorbed on nearby oxygen sites.
- INS spectroscopy identifies the γ(OH) and δ(OH) modes of residual hydroxyl groups on alumina, with difference spectra revealing the formation and consumption of hydroxyl groups as a consequence of the adsorption process. Correlation of the energy and momentum transfer characteristics for a band at 900–1000 cm^{-1}, assigned to δ(OH) of surface hydroxyl groups, confirms this feature to be a fundamental transition.
- The first overtone of δ(OH) undergoes a Fermi resonance interaction with ν(OH) of hydrogen bonded hydroxyl groups and chemisorbed water molecules to yield an Evans transmission window in the diffuse reflectance spectrum at 2257 cm^{-1}.
- Dissociative HCl adsorption with consequent formation of hydroxyl groups occurs over a range of active sites. Dissociative HCl adsorption plus the exchange of a surface hydroxyl by chlorine is associated exclusively with the medium–strong Lewis acid site, recently described for this surface [15]. The site selectivity for this particular process reflects the relative balance of the bond energy terms involved.

Acknowledgements

The EPSRC and Ineos Chlor Ltd. are thanked for the provision of industrial CASE postgraduate studentships (ARM and DTL). Rutherford Appleton Laboratory is thanked for access to neutron beam facilities. The Scottish Higher Education Funding Council is thanked for equipment funding via the award of a Research Development Grant. Professor Frederick Thibault-Starzyk (CNRS Laboratoire Catalyse & Spectrochimie, Caen) is thanked for helpful discussions on the topic of an Evans transmission window.

References

[1] J. Thomson, G. Webb, J.M. Winfield, J. Mol. Catal. 67 (1991) 117.
[2] J. Thomson, G. Webb, J.M. Winfield, J. Mol. Catal. 68 (1991) 347.
[3] A. Kytökivi, M. Lindblad, A. Root, J. Chem. Soc. Faraday Trans. 91 (1995) 941.
[4] A. Melchor, E. Garbowski, M.V. Mathieu, M. Primet, J. Chem. Soc. Faraday Trans. 82 (1) (1986) 1893.
[5] R.S. Drago, E.E. Getty, J. Am. Chem. Soc. 110 (1994) 3311.
[6] G. Clet, J.M. Goupil, D. Cornet, Bull. Soc. Chim. Fr. 134 (1997) 223.
[7] M. Tanaka, S. Ogasawara, J. Catal. 16 (1970) 157.
[8] J.B. Peri, J. Phys. Chem. 70 (1966) 1482.
[9] J.W. Elam, C.E. Nelson, M.A. Tolbert, S.M. George, Surf. Sci. 450 (2000) 64.
[10] S. Alavi, D.C. Sorescu, D.L. Thomson, J. Phys. Chem. B 107 (2003) 186.
[11] K. Weissermel, H.-J. Arpe, Industrial Organic Chemistry, third ed., VCH, Weinheim 1997, p. 55.
[12] D.S. MacIver, H.H. Tobin, R.T. Barth, J. Catal. 2 (1963) 485.
[13] A.J. Léonard, P.N. Semaille, J.J. Fripiat, J. Proc. Br. Ceram. Soc. 103 (1969) 103.
[14] C.N. Satterfield, Heterogeneous Catalysis in Industrial Practice, second ed., Krieger Publishing, Malabar, 1996, p. 114.
[15] D.T. Lundie, A.R. McInroy, R. Marshall, C. Mitchell, J.M. Winfield, C.C. Dudman, P. Jones, S.F. Parker, D. Lennon, J. Phys. Chem. B 109 (2005) 11592.
[16] B.M. Weckhuysen, Phys. Chem. Chem. Phys. 5 (2003) 4351.
[17] M.A. Banares, Catal. Today 100 (2005) 71.

[18] J.M. Chalmers, G. Dent, Industrial Analysis with Vibrational Spectrosopy, Royal Society of Chemistry, Cambridge, 1997, p. 153.
[19] S.F. Parker, J.W. Taylor, P. Albers, M. Lopez, G. Sextl, D. Lennon, A.R. McInroy, I.W. Sutherland, Vib. Spectrosc. 35 (2004) 179.
[20] A.R. McInroy, D.T. Lundie, J.M. Winfield, C.C. Dudman, P. Jones, S.F. Parker, J.W. Taylor, D. Lennon, Phys. Chem. Chem. Phys. 7 (2005) 3093.
[21] Ineos Chlor Ltd., Catalyst reference: 25867/19A.
[22] C.J. Mitchell, P. Jones, (Imperial Chemical Industries Plc, UK). Patent PCT Int. Appl. WO 2000076658 (2000).
[23] D. Lennon, D.R. Kennedy, G. Webb, S.D. Jackson, Stud. Surf. Sci. Catal. 146 (1999) 341.
[24] D.R. Kennedy, G. Webb, S.D. Jackson, D. Lennon, Appl. Catal. A Gen. 259 (2004) 109.
[25] M. Arai, A.D. Taylor, S.M. Bennington, Z.A. Bowden, in: W.S. Howells, A.K. Soper (Eds.), Recent Developments in the Physics of Fluids, Adam Hilger, Bristol, 1992, pp. F321–F328.
[26] C.N. Banwell, Fundamentals of Vibrational Spectroscopy, second ed., McGraw-Hill, UK, 1972, p. 74.
[27] G. Hertzberg, Molecular spectra and molecular stucture, Infrared and Raman Spectra of Polyatomic Molecules, II, 1991, p. 535.
[28] L.F. Keyser, G.W. Robinson, J. Chem. Phys. 44 (1966) 3225.
[29] X. Liu, R.E. Truitt, J. Am. Chem. Soc. 119 (1997) 9856.
[30] J.C. Evans, N. Wright, Spectrochim. Acta 16 (1960) 352; J.C. Evans, Spectrochim. Acta 18 (1962) 507.
[31] M.F. Claydon, N. Sheppard, Chem. Commun. (1969) 1431.
[32] S. Bratos, H. Ratajczak, J. Chem. Phys. 76 (1982) 77.
[33] A.G. Pelmenschikov, J.H.M.C. van Wolput, J. Jänchen, R.A. van Santen, J. Phys. Chem. 99 (1995) 3612.
[34] L. Kubelková, J. Kotrla, J. Florián, J. Phys. Chem. 99 (1995) 10285.
[35] R.-S. Zhou, R.L. Snyder, Acta Crystallogr. B47 (1991) 617.
[36] P.C.H. Mitchell, S.F. Parker, A.J. Ramirez-Cuesta, J. Tomkinson, Vibrational Spectroscopy with Neutrons with Applications in Chemistry, Biology, Materials Science and Catalysis, World Scientific, Singapore, 2005.
[37] M.J. Wax, R.R. Cavanagh, J.J. Rush, G.D. Stucky, L. Abrams, D.R. Corbin, J. Phys. Chem. 90 (1986) 532.
[38] L.M. Kustov, V.Y. Borovkov, B. Kazansky, J. Catal. 72 (1981) 149.
[39] J.C. Lavalley, M. Benistel, J.P. Gallas, J. Lamotte, G. Busca, V. Lorenzelli, J. Mol. Struc. 175 (1988) 453.
[40] P. Hoffman, E. Knözinger, Surf. Sci. 188 (1987) 181.
[41] J.-C. Li, J. Chem. Phys. 105 (1996) 6733.
[42] S.F. Parker, S.M. Bennington, G. Aufferman, W. Bronger, H. Herman, K.P.J. Williams, T. Smith, J. Am. Chem. Soc. 125 (2003) 11656.